Biointerface Research in Applied Chemistry
Platinum Open Access Journal (ISSN: 2069-5837)

Article
Volume 12, Issue 6, 2022, 8394 - 8405
https://doi.org/10.33263/BRIAC126.83948405

Synthesis, Crystal Structure and Theoretical Investigations of (3-(2-Chlorophenyl)-5-Tosyl-1,3,3a,4,5,9b-Hexahydroisoxazolo[4,3-c]Quinolin-3a-yl)Methanamine

Raj Rangarajan Kamaraj [1,*], Rajesh Subramani [1], Sugumar Paramasivam [2], Savithiri Sambandam [3], Bharanidharan Sarangapani [4]

[1] Department of Physics, Pachaiyappa's College for Men, Kancheepuram – 631 501, Tamilnadu, India; Email id: jsrkraj@gmail.com (R.R.K.); rajeshphdphy@gmail.com (R.S.);
[2] Department of Physics, Dhaanish Ahmed College of Engineering, Tambaram, Chennai – 601 301, Tamilnadu, India; Email id: sugumar17283@gmail.com (S.P.);
[3] Department of Chemistry, Karpagam Academy of Higher Education, Coimbatore – 641 021, Tamilnadu, India;.Email id: savithiri.chem@gmail.com (S.S.);
[4] Department of Physics, Agni College of Technology, Thalambur, Chennai – 600 130, Tamilnadu, India;.Email id: bharani.dharan0@gmail.com (B.S.);
* Correspondence: jsrkraj@gmail.com (R.R.K.);

Scopus Author ID56472386900
Received: 16.09.2021; Revised: 19.10.2021; Accepted: 22.10.2021; Published: 11.12.2021

Abstract: In the title compound (3-(2-chlorophenyl)-5-tosyl-1,3,3a,4,5,9b-hexahydroisoxazolo[4,3-c]quinolin-3a-yl)methanamine **(3-CPTHIQM)**, the Thorpe–Ingold effect causes the S atom's tetrahedral geometry to be deformed, with O-S-O and N-S-C angles diverging from ideal tetrahedral values. The crystal packing features C—H···O hydrogen-bond interactions.The supramolecular interactions were confirmed and quantified using Hirshfeld surface analysis. Quantum chemical calculations of sulfonamide are calculated at DFT/B3LYP/6-311++G(d,p) basis set. The NLO properties were calculated at the same level of theory. Furthermore, frontier molecular orbitals (FMOs) and molecular electrostatic potential (MEP) surfaces were calculated and analyzed in detail. In a molecular docking study, the investigated sulfonamide compound is evaluated as a new potential cancer inhibitor.

Keywords: XRD; Hirshfeld surfaces; NLO; HOMO-LUMO; MEP; molecular docking.

1. Introduction

In recent decades, sulfonamide compounds have been an important class of therapeutic agents in the recent medicinal field [1-10]. Sulfonamides are useful moieties found in many organic compounds and are applicable in medicine and a range of other fields [11-15]. Many therapeutic drugs contain the pharmacologically active component $–SO_2NH–$ found in sulfonamides [16].

Coumarins got an incredible interest in the literature from scientists, medicinal chemists, and drug specialists as a result of their energizing, flexible, and expansive range of natural exercises. Sulfonamide drugs are commonly used to treat infections caused by Gram-positive and Gram-negative bacteria and some fungi and protozoa. Anti-filarial action has been found in one of the Sulfonamide derivatives (epoxysulphonamides and ethynesulphonamides)

[17]. It is well known that administering sulfonamides in the form of metal complexes improves toxicological and pharmacological effects. The coordination chemistry of sulfonamides has undergone noticeable development in recent years due to the interesting properties of these substances. In this work, we synthesized novel sulfonamide derivatives containing nitro groups, the compounds characterized experimentally and theoretically using different techniques. X-ray diffraction studies determined the sulfonamide derivative, followed by intermolecular contact, fingerprint plots, and molecular surface contours (d_{norm}, di, and de) provided by Hirshfeld surface analysis. The DFT approach with the B3LYP/6-311++G(d,p) basis set was used to estimate theoretical investigations. In the light of the above importance and in further continuation of our this study to develop novel drug agents, the study is aimed to design, molecular docking, and synthesize of (3-(2-chlorophenyl)-5-tosyl-1,3,3a,4,5,9b-hexahydroisoxazolo[4,3-c]quinolin-3a-l)methanamine as prospective anticancer and antimicrobial agents.

2. Materials and Methods

2.1. Experimental details.

2.1.1. Synthesis procedure.

At room temperature, a solution of 4-chloro-1-tosyl-1,2-dihydroquinoline (1 mmol) and potassium carbonate (1.2 mmol) was agitated for 10 minutes. 2-chlorobenzaldehyde (1.2 mmol) and 2-aminoacetamide (1.2 mmol) were added dropwise to this solution until the addition was complete.

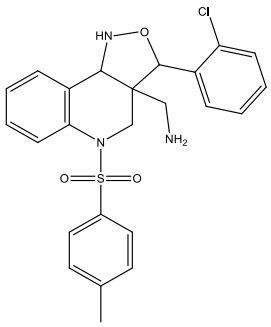

Scheme 1. The schematic representation of (3-(2-chlorophenyl)-5-tosyl-1,3,3a,4,5,9b-hexahydroisoxazolo[4,3-c]quinolin-3a-yl)methanamine.

After the finishing of the response, as demonstrated by TLC, acetonitrile has vanished. EtOAc (25 ml) and water (25 ml) were added to the unrefined mass. The natural layer was dried over anhydrous sodium sulfate. Expulsion of dissolvable prompted the unrefined item, which was sanitized through a stack of silica gel (100–200mesh) utilizing benzene and ethyl acetate and (9:1) as solvents.

The unadulterated title compound was gotten as a dreary strong (80% yield). Recrystallization was completed utilizing ethyl acetate as a dissolvable.

2.2. Computational details.

2.2.1. Hirshfeld analysis.

Crystal Explorer [18] was used to generate the surfaces mapped over d_{norm}, and electrostatic potential for the title compound. The contact distances of di and de from the

Hirshfeld surface to the nearest atom, inside and outside, respectively, enable the analysis of the intermolecular interactions through the mapping of d_{norm}. Two-dimensional fingerprint plots [19] indicate the intermolecular contacts in the crystal structure.

2.2.2. DFT calculation.

Theoretical calculations were performed using DFT method with B3LYP/6-311++G(d,p) level of basis set by Gaussian 09W [20] program package, invoking gradient geometry optimization [20]. In the present work, the DFT approach with 6-311++G(d,p) as a basis set for calculating molecular structure and energies of optimized structures was utilized. In addition, the NLO, HOMO-LUMO, and MEP surfaces were calculated at the same level of theory.

2.2.3. Target identification.

Kinase inhibitors are very efficient in cancer therapy, specifically targeting specific mutations that mainly drive tumorigenesis. Cyclin-dependent kinases (CDKs) are a group of critical administrative proteins that control diverse cell action and are fundamentally occupied with the cell cycle and record. It isn't is actually to be expected that numerous infections, particularly disease, are normal in their abnormal exercises, given the crucial organic capacities played by CDKs. Diverse cell cycle proteins like CDKs and cyclins actuate the improvement of the cell cycle as they are the principal controllers of the cell cycle. Past preliminaries have shown that sulfonamide derivatives therapy arrests cancer cells in the G2/M stage CDK activity enable the orderly transition between cell cycle stages.

2.2.4. Molecular docking.

Investigate the binding mode of the synthesized title compound and standard drugs with selected protein for cancer cell lines; molecular docking study was implemented against human colorectal carcinoma (PDB ID: 5FGK) [21], was retrieved from the protein data bank. The entire docking calculations were performed using the Autodock docking module program [22]. Essential hydrogen atoms, Kollman united atom type charges, and solvation parameters were added with the aid of AutoDock tools [23]. It performs flexible protein-ligand docking and searches for favorable interactions between one typically small ligand molecule and a typically larger protein molecule. Docking process, wherein protein preparation inhibited refinement is carried out with a maximum of 20 poses, wherein the side chains are optimized, and refinement of residues takes place if the ligand poses are within 5.0Å. The best-docked structure was chosen by docking score, and the number of amino acids matches (hydrogen bonds) with the original drug complex.

3. Results and Discussion

3.1. X-ray crystal structure.

Intensity data of the sulfonamide compound were collected using on a BRUKER KAPPA AREA diffractometer [24] at room temperature (296 °K) utilizing graphite-monochromated Mo-Kα radiation (λ = 0.71073 Å) by applying the X-scan process. Information assortment and cell refinement were done utilizing APEXS [24], while information decrease was applied utilizing SAINT [25]. The structures were solved using direct methods using

SHELXS97 [25] and refined with full-matrix least-squares calculations using SHELXL [25] implemented in the WinGX program suit. The molecular graphics for drawing ORTEP plots using PLATON [26].

The ORTEP plot of the title compound is displayed in Fig. 1. The sulfur atom S1 shows a distorted tetrahedral geometry, with O2—S1—O3 and N1—S1—C8 angles deviating from ideal tetrahedral values are attributed to the Thrope-Ingold effect. The sum of bond angles around N1 indicates that N1 is in sp^2 hybridization. The geometric parameters (bond length, bond angle, and torsion angles) agree well with those reported for similar structures [27, 28].

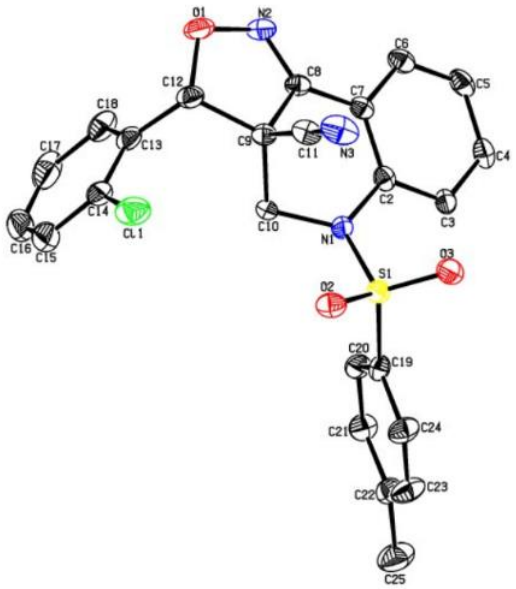

Figure 1. The structure of the title compound, showing 50% probability displacement ellipsoids.

3.2. DFT study.

3.2.1. NLO property.

NLO materials have been the subject of exceptional research because of their possible application in various technologies, like optical communication, optical computing, and data storage [29].

Accordingly, it is realized that there has been extreme investigation for molecules with large non-zero hyperpolarizabilities since these substances have potential as the constituents of NLO materials. The organic compound-containing systems are extraordinarily important among the many molecular designs used for introducing NLO behavior [30]. Due to their particular photoswitching properties, benzenes are utilized in numerous areas of molecular electronics and are suitable for various kinds of applications [31, 32].

In our case, the electronic dipole moment, molecular polarizability, anisotropy of polarizability, and molecular first hyperpolarizability of **3-CPTHIQM** were determined at the B3LYP/6-311++G(d,p) level of theory and are presented in Table 1. Notably, the higher values of dipole moment, molecular polarizability, and hyperpolarizability improve the NLO property. Urea is one of the prototypical molecules utilized to investigate the NLO property of molecular systems, and hence, it was used frequently as a threshold value for similar purposes. The first hyperpolarizability value of **3-CPTHIQM** was calculated as 24.29126×10^{-30}esu using the B3LYP/6-311++G(d,p) method. According to these results, the β_0 value of the present molecule is sixty-six times larger than the magnitude of urea.

Table 1. The NLO measurements of 3-CPTHIQM.

Parameters	**B3LYP/6-311++G(d,p)**
Dipole moment (μ)	**Debye**
μ_x	1.1287457
μ_y	0.7340742
μ_z	0.2543639
μ	1.37026 **Debye**
Polarizability (α_0)	**$x10^{-30}$esu**
α_{xx}	270.4608738
α_{xy}	21.7253486
α_{yy}	119.8610325
α_{xz}	-54.1047968
α_{yz}	-48.9291337
α_{zz}	355.2567156
α_0	0.50874**$x10^{-30}$esu**
Hyperpolarizability (β_0)	**$x10^{-30}$esu**
β_{xxx}	371.2653814
β_{xxy}	152.8269434
β_{xyy}	18.1346997
β_{yyy}	-14.8196612
β_{xxz}	-892.6269248
β_{xyz}	-255.2317476
β_{yyz}	-46.3674218
β_{xzz}	1765.1673739
β_{yzz}	217.3497354
β_{zzz}	-832.2519857
β_0	24.29126**$x10^{-30}$esu**

Standard value for urea (**μ**=1.3732 Debye, **β_0**=0.3728x10^{-30}esu): **esu**-electrostatic unit

3.2.2. HOMO - LUMO analysis.

The optimized molecular structure of **3-CPTHIQM** is shown in Figure 2. The Homo is localized on the quinoline amine group, and the Lumo is located on the tosyl group, as shown in Figure 3. The transition from Homo to Lumo is simpler than Homo-1 to Lumo+1. This phenomenon explains why the lowest energy absorption is a charge transfer transition from Homo to Lumo and an electronic transition.

In this way, the electron density decreases in the electron-donating azo when electrons transfer from the HOMO to LUMO. This phenomenon is accompanied by an increase in the electron density of the electron accepting the moiety. This result demonstrates that the electrons transfer from the unit of the propionate moiety. The Homo and Lumo energies for sulfonamide were calculated at -5.95055 eV and -2.09408 eV, respectively, whereas the Homo-Lumo energy gap is 3.85647 eV.

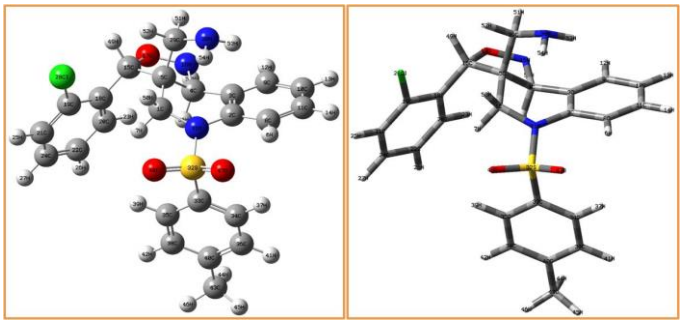

Figure 2. The optimized molecular structure of 3-CPTHIQM.

In addition to this, the various physicochemical parameters such as ionization potential (IP), electron affinity (EA), electrophilicity index (ω), chemical potential (μ), electronegativity

(χ), and hardness (η) were calculated by using the standard procedure [33] and are presented in Table 2.

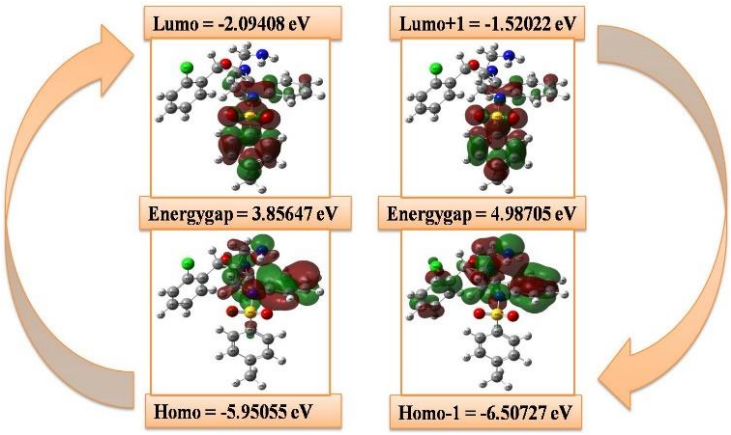

Figure 3. The Frontier molecular orbitals of 3-CPTHIQM.

Table 2. The Physico-chemical properties of 3-CPTHIQM.

Parameters	Values
HOMO	-5.95055 eV
LUMO	-2.09408 eV
(Homo – Lumo) Energy gap	3.85647 eV
HOMO-1	-6.50727 eV
LUMO+1	-1.52022 eV
(Homo-1 – Lumo+1) Energy gap	4.98705 eV
Ionization potential (IP)	5.95055 eV
Electron affinity (EA)	2.09408 eV
Electrophilicity Index (ω)	2.09765
Chemical Potential (μ)	4.02232
Electronegativity (χ)	-4.02232
Hardness (η)	-3.85647

3.2.3. MEP analysis.

The MEP is a plot of molecule electrostatic potential projected on a constant electron density surface that shows molecular size and shape as well as electrostatic potential value in terms of color grading. The MEP might be utilized to distinguish regions on the surface that are electron-rich (electrophilic attack) from those which are electron-poor (nucleophilic attack) and has been viewed as an extremely helpful tool in the investigation of the correlation between molecular structure and the physio-chemical property relationship of molecules including bio-molecules and drugs [34, 35].

The MEP surface map was determined at the B3LYP/6-311++G(d,p) basis set. It is identified with the electronic density, and it is an extremely valuable descriptor in understanding sites for electrophilic attacks and nucleophilic reactions as well as hydrogen bonding interactions [36]. The importance of MEP lies in the fact that it simultaneously displays molecular size, shape, and positive, negative, and neutral electrostatic potential regions in terms of color grading, as shown in Figure 4. Potential increases in the order red < orange < yellow < green < blue. The color code of blue indicates the strongest interaction, and red indicates the strongest repulsion. The negative V(r) regions are usually associated with the lone pair of electronegative atoms (oxygen and nitrogen); the regions having the positive potential are over the hydrogen atoms. From these results, we can say that the hydrogen atoms indicate the strongest attraction, and oxygen, nitrogen, and sulfur atoms indicate the strongest repulsion.

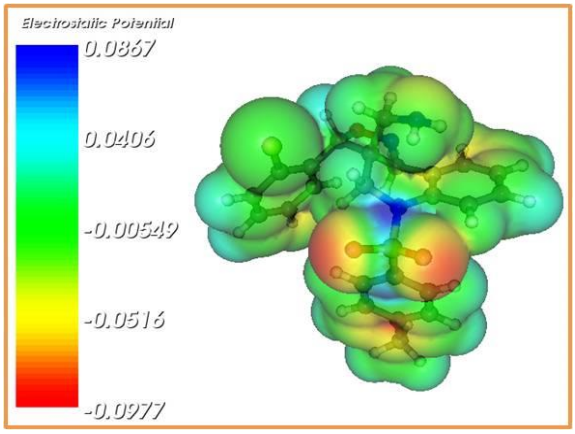

Figure 4. The MEP surface of 3-CPTHIQM.

3.3. Hirshfeld surface analysis.

The hydrogen-bonding network generated in the crystal can be visualized using Hirshfeld surface analysis. The bright-red spots on the Hirshfeld surface mapped over d_{norm} as shown in Figure 5.

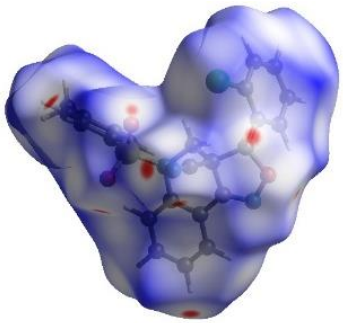

Figure 5. d_{norm} mapped on the Hirshfeld surface for visualizing the contacts of the title compound. Dotted lines indicate hydrogen bonds.

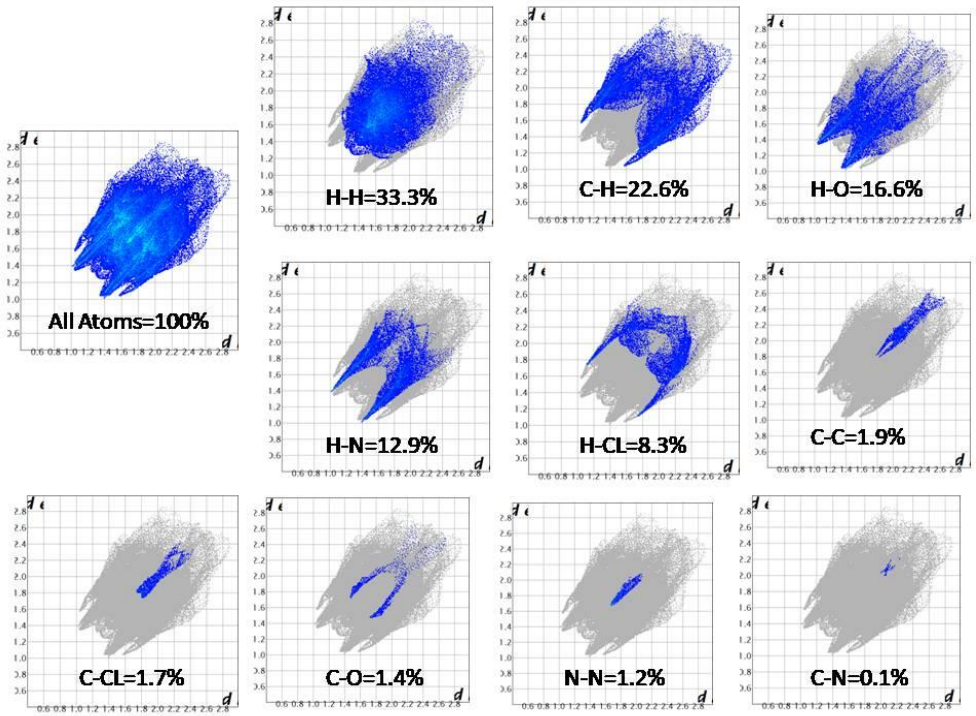

Figure 6. Fingerprint plot of the title compound. The outline of the full fingerprint plots is shown in grey. Di is the closest internal distance from a given point on the Hirshfeld surface, and de is the closest external contact.

The overall two-dimensional fingerprint plot is illustrated in Figure 6, and those are delineated into H-H;C-H/H-C; H-O/O-H; H-N/N-H; H-CL/CL-H; C-C; C-CL/CL-C; C-O/O-C; N-N and C-N/N-C, respectively. The highest contribution to the overall Hirshfeld surface, i.e., 33.3%, is H-H contacts. The other relative contributions of the other different intermolecular interactions to the Hirshfeld surface are shown in descending order are H-H=33.3%, C-H=22.6%, H-O=16.6%, H-N=12.9%, H-CL=8.3%, C-C=1.9%, C-CL=1.7%, C-O=1.4%, N-N=1.2%, and C-N=0.1%, respectively.

3.4. Molecular docking study.

The synthesized derivatives of the title compound showed tremendous molecular docking results, and the selected proteins were discovered to correspond with significant amino acids residues. Molecular docking was performed to analyze the best binding mode of active sulfonamide compounds for the cancer cell lines of human colorectal carcinoma.

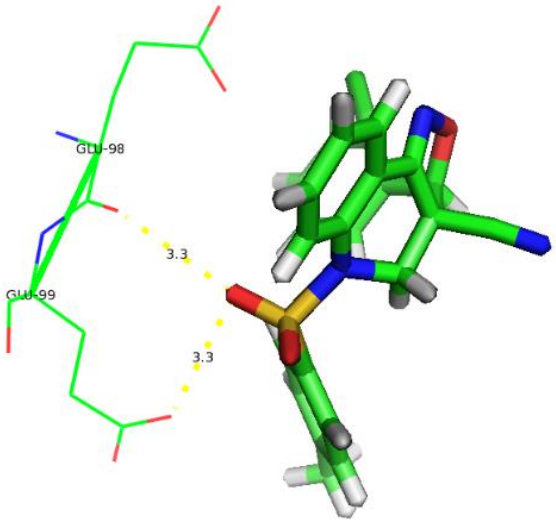

Figure 7. Binding surface and ligand interaction diagram of the title compound with their respective targeted protein.

The docked, glide energy, and hydrogen bonding interactions of the title compound and co-crystallized ligand are given in Table 3. A view of the X-ray crystal structure of the title compound in the human colorectal carcinoma receptor active site showing the key hydrogen contacts between inhibitor and enzyme is depicted in Figures 7 and 8. The surface diagram showing the title compound docked at the active site of the human colorectal carcinoma receptor is depicted in Figure 9.

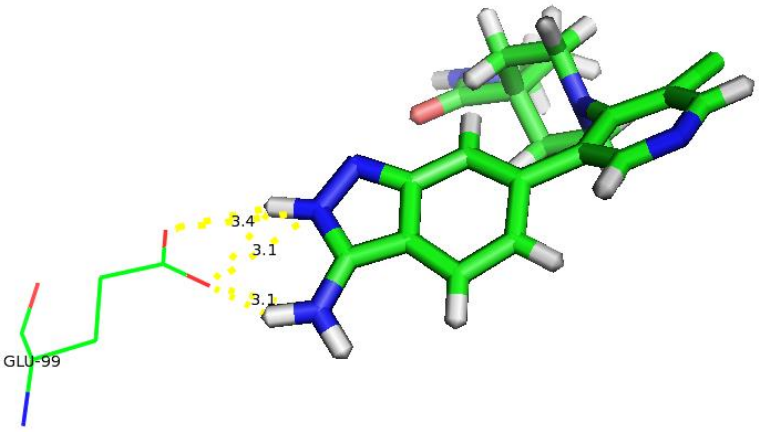

Figure 8. Binding surface and ligand interaction diagram of native ligand (cocrystal) with their respective protein.

Molecular analysis of sulfonamide compound indicated that hydrogen bond and hydrophobic are four major interactions (GLU98 and GLU99) incorporating the attachment of this ligand to human colorectal carcinoma Inhibitors acceptor.

Table 3. Hydrogen bond interactions of the title compound with amino acids at the active site of human colorectal carcinoma Receptor.

Compound	Docking score	Hydrogen bonding interactions		
		Donor	Acceptor	Distance Å
3-CPTHIQM	-6.4	O-H[GLU98] O-H[GLU99]	O* O*	**3.3** **3.3**
Co-Crystal	-6.1	O[GLU99] O[GLU99]	N-H* N-H*	3.3 3.1

The co-crystallized ligand also docked well, and it shows better interactions with active residues. The results show that the title compound has better binding energy, and the co-crystallized ligand has comparable interactions. Docking results and interacting residues are shown in Table 3.

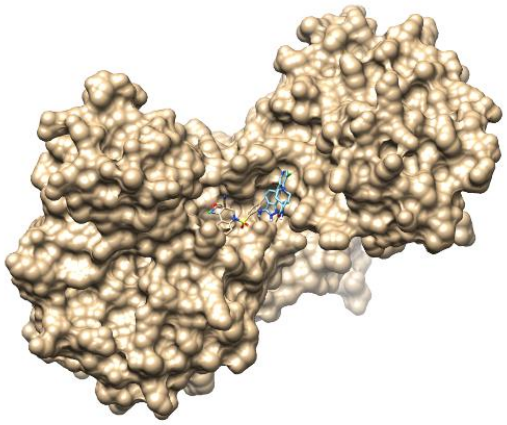

Figure 9. Binding surface and ligand interaction diagram of the title compound.

The docking findings, therefore, indicate that the synthesized title compound may be of excellent importance in effective chemotherapy. The X-ray crystal structures confirmed the expected binding mode and considered the binding orientation. Electronic properties made optimizing the title compound a more potent second-generation lead.

4. Conclusions

The important biological compound has been studied by theoretical and experimental methods. The title compound has been confirmed by an X-ray diffraction study. Besides, the first hyperpolarizability value of the molecule is found to be high, i.e., sixty-six times greater than that of urea; hence the NLO activity of the molecule will also be proportionately high. The energy gap (3.85647 eV) determines the stability and reactivity of the title molecule, according to the HOMO-LUMO analysis. MEP surface analysis of the active charge sites of the title molecule. The physicochemical properties were calculated and analyzed. Some approaches to quantum chemical modeling of possible interaction of the title molecule with receptors have been used.

Funding

This research received no external funding.

Acknowledgments

This research has no acknowledgment.

Conflict of Interest

The authors declare no conflicts of interest.

References

1. Meseli, T.; Dogan, Ş.D.; Gundüz, M.G.; Kokbudak, Z.; Skaro Bogojevic, S.; Noonan, T. Design, synthesis, antibacterial activity evaluation and molecular modeling studies of new sulfonamides containing a sulfathiazole moiety. *New Journal of Chemistry*, **2021**, *45*, 8166–8177, http://dx.doi.org/10.1039/d1nj00150g.
2. Onoabedje, E.A.; Ibezim, A.; Okoro, U.C.; Batra, S. New sulphonamide pyrolidine carboxamide derivatives: Synthesis, molecular docking, antiplasmodial and antioxidant activities. *PLOS ONE*, **2021**, *16*,http://dx.doi.org/10.1371/journal.pone.0243305.
3. Pradhan, S.; Prasad, R.; Sinha, C.; Sen, P. Molecular modeling of potent novel sulfonamide derivatives as non-peptide small molecule anti-COVID 19 agents. *Journal of Biomolecular Structure and Dynamics*, **2021**, 1–14, http://dx.doi.org/10.1080/07391102.2021.1897043.
4. Irfan, A.; Ahmad, S.; Hussain, S.; Batool, F.; Riaz, H.; Zafar, R. Recent Updates on the Synthesis of Bioactive Quinoxaline-Containing Sulfonamides. *Applied Sciences*, **2021**, *11*, 5702, http://dx.doi.org/10.3390/app11125702.
5. Raj, R.K.; Rajesh, S.; Sugumar, P.; Bharanidharan, S.; Savithiri, S. Crystal structure, Hirshfeld surface, DFT and molecular docking studies of (z)-methyl 2-((n-(2-formylphenyl)-4-methylphenylsulfonamido)methyl)-3-(4-methoxyphenyl)acrylate. *Journal of Advanced Scientific Research*, **2021**, *12*, 104-112.
6. Cinar, E.B.; Faizi, M.S.H.; Yagci, N.K.; Dogan, O.E.; Aydin, A.S.; Agar, E.; Dege, N.; Mashrai, A. Crystal structure, Hirshfeld surface analysis and DFT studies of (E)-4-methyl-2-{[(2-methyl-3-nitro-phen-yl)imino]-meth-yl}phenol. *Acta crystallographica. Section E, Crystallographic communications*, **2020**, *76*, 1551-1556, http://doi.org/10.1107/s2056989020011652.
7. Irfan, A.; Rubab, L.; Rehman, M.U.; Anjum, R.; Ullah, S.; Marjana, M. Coumarin sulfonamide derivatives: An emerging class of therapeutic agents. *Heterocyclic Communications*, **2020**, *26*, 46–59, http://dx.doi.org/10.1515/hc-2020-0008.
8. Onoabedje, E.A.; Ibezim, A.; Okoro, U.C.; Batra, S. Synthesis, molecular docking, antiplasmodial and antioxidant activities of new sulfonamido-pepetide derivatives. *Heliyon*, **2020**, *6*, e04958, http://dx.doi.org/10.1016/j.heliyon.2020.e04958.
9. Zhang, A.; Li, W.; Liu, X.; Wu, M.; Xuan, G. Synthesis, Biological Evaluation and in Silico Studies of Several Substituted Benzene Sulfonamides as Potential Antibacterial Agents. *Journal of Physics: Conference Series*, **2020**, *1624*, 022058, http://dx.doi.org/10.1088/1742-6596/1624/2/022058.
10. Mary, S.J.J.; Siddique, M.U.M.; Pradhan, S.; Jayaprakash, V.; James, C. Quantum chemical insight into molecular structure, NBO analysis of the hydrogen-bonded interactions, spectroscopic (FT–IR, FT–Raman), drug likeness and molecular docking of the novel anti COVID-19 molecule 2-[(4,6-diaminopyrimidin-2-yl)sulfanyl]-N-(4-fluorophenyl)acetamide - dimer. *Spectrochimica Acta Part A: Molecular and Biomolecular Spectroscopy*, **2021**, *244*, 118825, http://dx.doi.org/10.1016/j.saa.2020.118825.
11. Park, H.B.; Wei, Z.; Oh, J.; Xu, H.; Kim, C.S.; Wang, R. Sulfamethoxazole drug stress upregulates antioxidant immunomodulatory metabolites in Escherichia coli. *Nature Microbiology*, **2020**, *5*, 1319–1329, http://dx.doi.org/10.1038/s41564-020-0763-4.
12. Gaballah, S.; Amer, H.; Hofinger-Horvath, A.; Al-Moghazy, M.; Hemida, M.I. Synthesis, Antimicrobial, and Docking Investigations of Remarkably Modified Sulfathiazole Derivatives. *Egyptian Journal of Chemistry*, **2020**, *63*, 171–184, http://dx.doi.org/10.21608/ejchem.2019.13909.1862.
13. Zhang, W.; Wei, Z.; Huang, G.; Xie, F.; Zheng, Z.; Li, S. Study of triaryl-based sulfamic acid derivatives as HPTPβ inhibitors. *Bioorganic & Medicinal Chemistry*, **2020**, *28*, 115777, http://dx.doi.org/10.1016/j.bmc.2020.115777.

14. Wu, P.; Ren, H. Azobenzene with sulfonamide group deprotonated by green developer for moisture detection and water jet rewritable paper. *Dyes and Pigments*, **2021**, *196*, 109764, http://dx.doi.org/10.1016/j.dyepig.2021.109764.
15. Sovari, S.N.; Vojnovic, S.; Bogojevic, S.S.; Crochet, A.; Pavic, A.; Nikodinovic-Runic, J. Design, synthesis and in vivo evaluation of 3-arylcoumarin derivatives of rhenium(I) tricarbonyl complexes as potent antibacterial agents against methicillin-resistant Staphylococcus aureus (MRSA). *European Journal of Medicinal Chemistry*, **2020**, *205*, 112533, http://dx.doi.org/10.1016/j.ejmech.2020.112533.
16. Abbasi, M.A.; Mujahid, U.; Aziz-ur-Rehman.; Rasool, S.; Khan, K.M.; Ashraf, M. Synthesis of Some N-Substituted Sulfonamides Derived from Moringine as Lipoxygenase Inhibitors. *Pakistan Journal of Chemistry*, **2014**, *4*, 161–166, http://dx.doi.org/10.15228/2014.v04.i04.p02.
17. Trigunait, A.; Damodharan, K.; Manickam, B.; Krishnasamy, G. Crystal structure of methyl (2Z)-2-{[N-(2-formylphenyl)-4-methylbenzenesulfonamido]methyl}-3-(4-methoxy phenyl)prop-2-enoate. *Acta Crystallographica Section E Crystallographic Communications*, **2015**, *71*, o1088–o1089, http://dx.doi.org/10.1107/s2056989015024172.
18. Wolff, S.K.; Grimwood, D.J.; McKinnon, J.J.; Turner, M.J.; Jayatilaka, D.; Spackman, M.A. *CrystalExplorer, Version 3.0.*, University of Western Australia, **2012**.
19. Rohl, Andrew L.; Massimo Moret.; Werner Kaminsky.; Kacey Claborn.; Joshua J. McKinnon.; Bart Kahr. Hirshfeld Surfaces Identify Inadequacies in Computations of Intermolecular Interactions in Crystals: Pentamorphic 1,8-Dihydroxyanthraquinone. *Crystal Growth & Design*, **2008**, *8*, 4517–4525, http://dx.doi.org/10.1021/cg8005212.
20. Frisch, M.J.; Trucks, G.W.; Schlegel, H.B.; Scuseria, G.E.; Robb, M.A.; Cheeseman, J.R.; Scalmani, G.; Barone, V.; Mennucci, B.; Petersson, G.; Nakatsuji, H. *Gaussian 09, Revision d. 01, Gaussian. Inc.*, Wallingford CT, **2009**.
21. Mallinger, A.; Schiemann, K.; Rink, C.; Stieber, F.; Calderini, M.; Crumpler, S. Discovery of Potent, Selective, and Orally Bioavailable Small-Molecule Modulators of the Mediator Complex-Associated Kinases CDK8 and CDK19. *Journal of Medicinal Chemistry (ACS)*, **2016**, *59*, 1078–1101, http://dx.doi.org/10.1021/acs.jmedchem.5b01685.
22. Bikadi, Z.; Hazai, E. Application of the PM6 semi-empirical method to modeling proteins enhances docking accuracy of AutoDock. *Journal of Cheminformatics*, **2009**, *1*,http://dx.doi.org/10.1186/1758-2946-1-15.
23. Garrett M. Morris.; David S. Goodsell.; Robert S. Halliday.; Ruth Huey, William E. Hart, Richard K. Belew, Arthur J. Olson. Automated docking using a Lamarckian genetic algorithm and an empirical binding free energy function. *Journal of Computational Chemistry*, **1998**, *19*, 1639-1662, https://doi.org/10.1002/(SICI)1096-987X(19981115)19:14<1639::AID-JCC10>3.0.CO;2-B.
24. SAINT. *Data Reduction and Correction Program. v. 8.27B.* Bruker AXS Inc., Madison, Wisconsin, USA, **2012**.
25. Sheldrick, G.M. A short history of SHELX. *Acta Crystallographica Section A Foundations of Crystallography*, **2007**, *64*, 112–122, http://dx.doi.org/10.1107/s0108767307043930.
26. Spek, A.L. Structure validation in chemical crystallography. *Acta Crystallographica Section D Biological Crystallography*, **2009**, *65*, 148–155, http://dx.doi.org/10.1107/s090744490804362x.
27. Ranjith, S.; Sugumar, P.; Sureshbabu, R.; Mohanakrishnan, A.K.; Ponnuswamy, M.N. Ethyl 2-[N-(2-formylphenyl)benzenesulfonamido]acetate. *Acta Crystallographica Section E Structure Reports*, **2009**, *65*, http://dx.doi.org/10.1107/s160053680900292x.
28. Madhanraj, R.; Murugavel, S.; Kannan, D.; Bakthadoss, M. Methyl (Z)-2-{[N-(2-formylphenyl)-4-methylbenzenesulfonamido]methyl}-3-phenylprop-2-enoate. *Acta Crystallographica Section E Structure Reports*, **2011**, *67*, http://dx.doi.org/10.1107/s1600536811050756.
29. Andraud, C.; Zabulon, T.; Collet, A.; Zyss, J. Nonlinear optical properties of polyenoctupoles: a multipolar tensorial quantum analysis. *Chemical Physics*, **1999**, *245*, http://dx.doi.org/10.1016/s0301-0104(99)00080-4.
30. Xie, S.; Natansohn, A.; Rochon, P. Recent developments in aromatic azo polymers research. *Chemistry of Materials (ACS)*, **1993**, *5*, 403–411, http://dx.doi.org/10.1021/cm00028a003.
31. Ikeda, T.; Tsutsumi, O. Optical Switching and Image Storage by Means of Azobenzene Liquid-Crystal Films. *Science (AAAS)*, **1995**, *268*, 1873–1875, http://dx.doi.org/10.1126/science.268.5219.1873.
32. Kawata, S.; Kawata, Y. Three-Dimensional Optical Data Storage Using Photochromic Materials. *Chemical Reviews (ACS)*, **2000**, *100*, 1777–1788, http://dx.doi.org/10.1021/cr980073p.
33. Bharanidharan, S.; Saleem, H.; Nathiya, A.; Arokiasamy, A.; Thanikachalam, V. Spectroscopic Investigations of (E)-5-(2-Phenyldiazenyl)-2-Hydroxybenzaldehyde Using DFT Method. *International*

Letters of Chemistry, Physics and Astronomy, **2015**, *60*, 168–181, http://dx.doi.org/10.18052/www.scipress.com/ilcpa.60.168.
34. Murray, J.S.; Sen, K. Molecular Electrostatic Potentials, Concepts and Applications. Elsevier, Amsterdam, **1996**.
35. Scrocco, E.; Tomasi, J.; Lowdin, P. Advances in Quantum Chemistry. Academic Press, New York, **1978**.
36. Luque, F.; López, J.; Orozco, M. Perspective on Electrostatic interactions of a solute with a continuum. A direct utilization of ab initio molecular potentials for the prevision of solvent effects. *Theoretical Chemistry Accounts*, **2000**, *103*, 343–345, https://doi.org/10.1007/s002149900013.